

# Research of Low Loss Intelligent Reflecting Surface Based on Liquid Crystal Technology

Yue CUI<sup>†</sup>, Hiroyasu SATO<sup>†</sup>, Hideo FUJIKAKE<sup>†</sup>, and Qiang CHEN<sup>†</sup>

<sup>†</sup> Department of Communications Engineering, Tohoku University  
Katahira 2-1-1, Aoba-ku, Sendai, 980-8579, Japan.

E-mail: †cui.yue.t4@dc.tohoku.ac.jp

**Abstract** In this paper, we investigate methods to reduce reflection loss in liquid crystal intelligent reflecting surfaces (LCIRS). First, we propose a novel structure that minimizes the reflection loss by eliminating the electric field within the liquid crystal (LC). By introducing an air layer into the intelligent reflecting surface (IRS) configuration and adjusting its thickness, the electric field can be effectively controlled. Experimental results demonstrate a reduction in reflection loss of up to 8.8 dB, although this approach also leads to a decrease in the reflection phase change. To overcome the phase change limitation, we propose a bias voltage supply method. In this approach, the resonant structures of the LCIRS element are independently connected to bias lines, allowing for separate control of two distinct resonances. Measurements indicate that this method can achieve a reduction in reflection loss of up to 17 dB while maintaining a 570-degree phase change, thereby validating its effectiveness in mitigating reflection loss without compromising phase performance.

**Key words** Liquid crystal, phase change, intelligent reflecting surface, reflection loss.

## 1. Introduction

Intelligent reflecting surfaces (IRS) have emerged as an effective means to enhance electromagnetic signal strength in target areas without the need for additional base stations. Their planar configuration facilitates seamless integration into building facades and interior walls. To accommodate complex coverage requirements, IRS capable of dynamic beam steering has garnered widespread attention. Numerous studies have explored various IRS implementations—ranging from diode-based and mechanical approaches to the use of nematic liquid crystals (LC) [1–4]. The rod-like molecular structure of nematic LCs can be continuously reoriented by external electric or magnetic fields, leading to corresponding variations in permittivity. This property enables continuous beam steering, which is the primary advantage of liquid crystal intelligent reflecting surfaces (LCIRS). Moreover, the ease of applying external electric fields via bias lines further contributes to the design simplicity and cost-effectiveness of LCIRS.

However, LCIRS exhibits a notable disadvantage in the form of high reflection loss. This loss not only dissipates the incident electromagnetic energy but also causes significant variations in the reflection magnitude across different reflection phases, ultimately reducing the aperture efficiency of the LCIRS [5]. To mitigate this issue, a novel structure is proposed that incorporates an air layer beneath the LC layer. Both simulation and experimental results indicate that the thickness of the air layer critically influences reflection loss and variation in reflection magnitude. In addition, a cost-effective 3D-printed fixture is employed to precisely control the air layer thickness. While the proposed LCIRS structure offers reduced reflection loss, low cost, and ease of fabrication, it comes with the trade-off that the reflection phase change decreases as the loss is minimized.

To mitigate reflection loss without compromising the phase change, we propose a novel RIS-LC unit cell employing a dual-

bias voltage supply method. In this design, two bias lines independently control the LC permittivities beneath two resonant structures of different sizes, allowing separate tuning of each resonance. This approach enables one reflection phase to correspond to multiple reflection magnitudes, thereby facilitating the selection of optimal magnitudes across all phases. As a result, the proposed RIS-LC structure achieves a reduction in reflection loss while maintaining a wide phase change, all within a simple and efficient design.

## 2. Air Layer Introduced LCIRS

### 2.1 Proposed structure

Fig. 1 illustrates the proposed LCIRS unit cell structure, which comprises five layers arranged from top to bottom: the superstrate, the LC layer, the substrate, the air layer, and the metal ground. Two identical metal patches are located on the upper and lower surfaces of the LC layer, with each patch connected to a bias line for voltage application. In the absence of bias voltage, the LC exhibits a relative permittivity of  $\epsilon_{r\perp} = 2.5$  and a loss tangent of  $\tan \delta_{\perp} = 0.02$ . Conversely, under full bias, these values change to  $\epsilon_{r\parallel} = 3$  and  $\tan \delta_{\parallel} = 0.007$ , respectively. Additionally, to ensure a smooth surface for the polyimide film coating process, glass (with  $\epsilon_r = 3.7$  and  $\tan \delta = 0.007$ ) is used as the material for both the superstrate and the substrate.

### 2.2 Theoretical Analysis

When electromagnetic waves propagate through a dielectric medium, a portion of their energy is dissipated due to the material's inherent conductivity ( $\sigma$ ) [6].

$$P_{loss} = \frac{\sigma}{2} \iiint_v |\mathbf{E}|^2 dv \quad (1)$$

where  $P_{loss}$  represents the time-averaged dissipated power. In LCIRS, the dissipation of incident energy within the LC layer—as

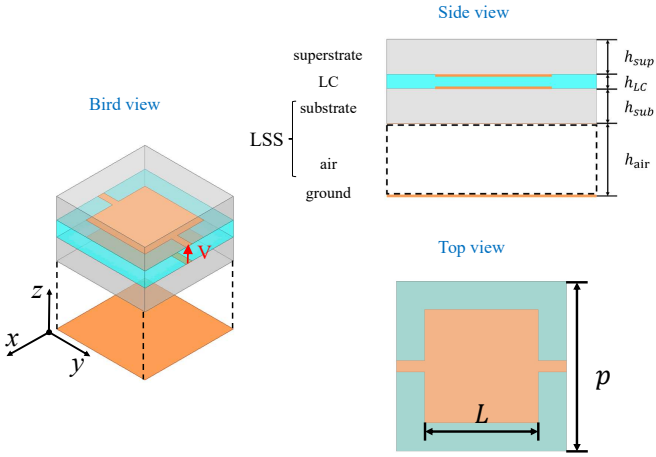


Fig. 1 The proposed LCIRS unit cell structure.

well as in other substrates and metals—is termed reflection loss. Due to the high loss tangent,  $\tan \delta = \sigma / \omega \epsilon$ , exhibited by the LC, the reflection loss is predominantly attributed to energy dissipation within the LC. To mitigate this issue, the proposed LCIRS unit cell incorporates an air layer beneath the LC layer. This design effectively reduces the electric field intensity while maintaining a thin LC layer, all without incurring additional costs.

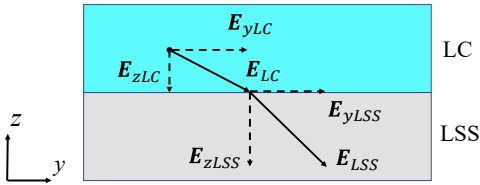


Fig. 2 The schematic of electric field at the interface between the LC layer and the substrate.

When a plane electromagnetic wave illuminates the proposed LCIRS, the metal patch induces a current that subsequently excites an electric field [7]. For clarity, the substrate and air layer are collectively referred to as the loss suppression structure (LSS). Fig. 2 illustrates a schematic of the electric field at the interface between the LC layer and the LSS.  $E_y$  and  $E_z$  are used to represent the parallel and perpendicular component of the electric field. According to the Maxwell-Faraday equation and Gauss's law [8], the parallel and perpendicular components at the interface can be expressed as:

$$|E_{yLC}| = |E_{yLSS}| \quad (2)$$

$$\frac{\epsilon_{LSS}}{\epsilon_{LC}} = \frac{|E_{zLC}|}{|E_{zLSS}|} \quad (3)$$

where  $\epsilon_{LC}$  and  $\epsilon_{LSS}$  denote the permittivity of the LC and the effective permittivity of the LSS. The electric field intensity within the LC layer decreases as  $\epsilon_{LSS}$  is reduced, which can be achieved by adjusting the thickness of the air layer ( $h_{air}$ ):

$$\epsilon_{LSS} = \frac{(h_{sub} + h_{air})\epsilon_{sub}\epsilon_{air}}{h_{sub}\epsilon_{air} + h_{air}\epsilon_{sub}} \quad (4)$$

where  $\epsilon_{sub}$  and  $\epsilon_{air}$  represent the permittivity of the substrate and the air layer, respectively. Increasing the thickness of the air

layer ( $h_{air}$ ) reduces  $\epsilon_L$ , causing it to converge to  $\epsilon_0$ . Consequently, both the electric field in the LC layer and the reflection loss of the proposed LCIRS decrease with increasing  $h_{air}$ .

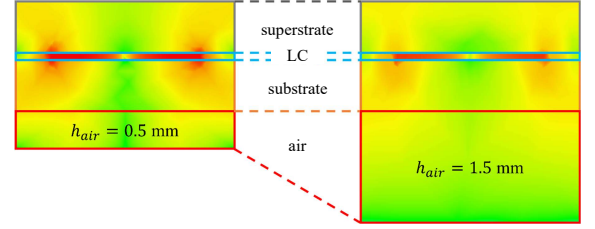


Fig. 3 The simulated electric field of the proposed LCIRS unit cell.

The aforementioned theoretical analysis was validated using full-wave simulations. Fig. 3 illustrates the simulated electric field for various air layer thicknesses. As  $h_{air}$  increases from 0.5 mm to 1.5 mm, the electric field within the LC layer decreases, which is consistent with the theoretical analysis. This reduction in the LC layer's electric field leads to a decrease in reflection loss.

### 2.3 Measurement

A  $15 \times 15$  prototype LCIRS was fabricated, consisting of three main components: the superstructure, the metal ground, and 3D printed fixtures, as shown in Fig. 4(a). The superstructure comprises the superstrate, the LC layer, and the substrate. Fig. 4(b) presents a side view of the assembled LCIRS, where the air layer is formed by the 3D printed fixtures, whose thickness can be adjusted by employing different fixtures.

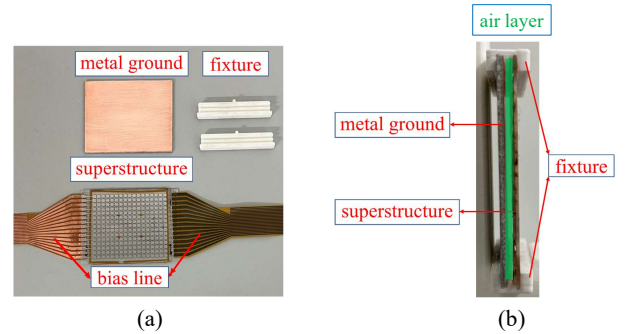
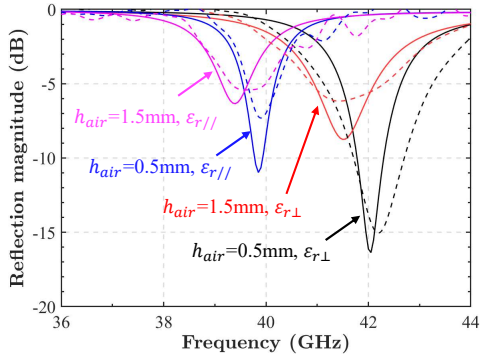


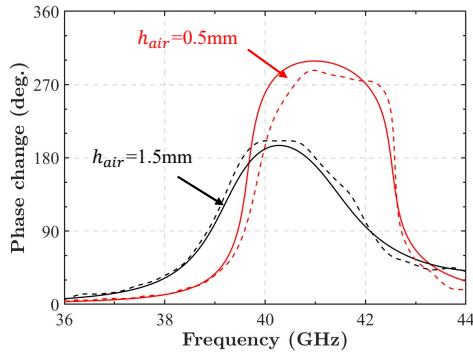
Fig. 4 (a) Unassembled and (b) side view of the assembled prototype LCIRS.

Fig. 5 presents the measurement results for various air layer thicknesses. As shown in Fig. 5(a), increasing  $h_{air}$  leads to a reduction in reflection loss. Specifically, compared to  $h_{air} = 0.5$  mm, an 8.8 dB reduction in reflection loss is observed when no bias voltage is applied ( $\epsilon_{r\perp}$ ), and a 3 dB reduction is achieved at full bias voltage ( $\epsilon_{r\parallel}$ ). Fig. 5(b) indicates that the reflection phase change decreases from 290 degrees to 204 degrees as  $h_{air}$  increases from 0.5 mm to 1.5 mm.

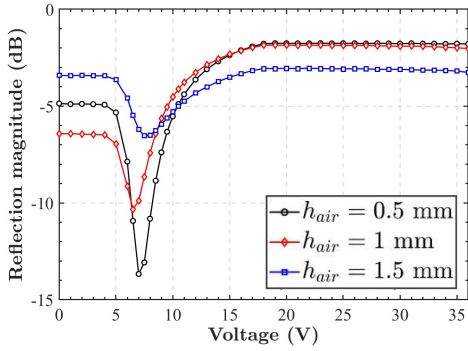
The reflection magnitude and phase versus bias voltage were measured to evaluate the proposed LCIRS structure, as shown in Fig. 5(c) and (d). The frequency was fixed at 40.3 GHz, and the air layer thicknesses were selected as 0.5 mm, 1 mm, and 1.5 mm, respectively. The variation in reflection magnitude decreased from 11.9 dB at  $h_{air} = 0.5$  mm to 3.4 dB at  $h_{air} = 1.5$  mm. Similarly, the phase variation reduced from 275 degrees at  $h_{air} = 0.5$  mm to 204 degrees at  $h_{air} = 1.5$  mm. These measured results validate the effectiveness of the proposed structure in reducing the reflection loss



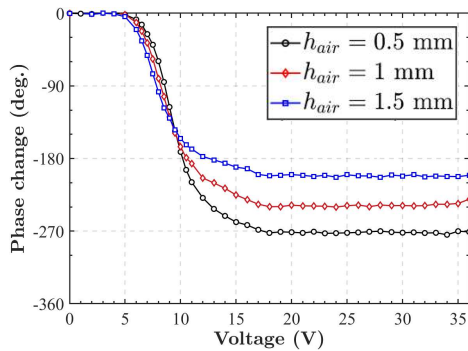
(a)



(b)



(c)



(d)

Fig. 5 Measured (a) reflection magnitude and (b) reflection phase change versus frequency, (c) reflection magnitude and (d) reflection phase versus bias voltage at 40.3 GHz.

of LCIRS, while also revealing a trade-off between reflection loss and phase change.

### 3. Dual-bias Voltage Supply Method

#### 3.1 Proposed structure

To address the trade-off between reflection loss and phase change, an alternative IRS element is proposed. The LCIRS unit structures employing the proposed dual bias supply method and the conventional single bias supply method are illustrated in Fig. 6. Both designs consist of a superstrate layer, an LC layer, and a metal ground. The single bias voltage supply method utilizes one bias line to control both resonant structures, whereas the proposed method employs two independent bias lines, enabling separate control of the two resonant structures via different bias voltages ( $V_1$  and  $V_2$ ), as shown in Fig. 6(a). The LC material and the superstrate material are the same as those used in the previously proposed element.

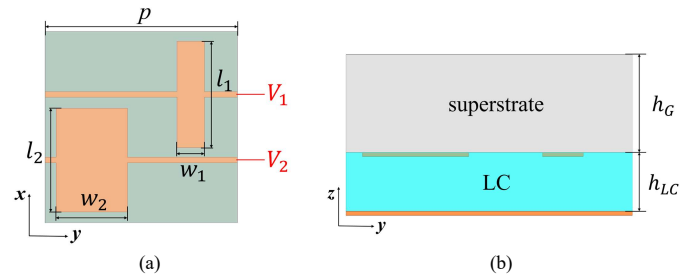


Fig. 6 Top view of the (a) single bias voltage supply method and the proposed method. (c) Side view of the LCIRS unit cell.

#### 3.2 Measurement and discussions

A  $12 \times 13$  LCIRS prototype, controlled by the proposed dual bias voltage supply method, was fabricated. The prototype is shown in Fig. 7(a), and the responses of the LC under different bias voltages  $V_1$  and  $V_2$  are presented in Fig. 7(b). It can be observed that the edges of the two resonant structures brighten individually, indicating that they are controlled independently.

Fig. 8 illustrates the measured performance of the single and dual bias voltage supply methods at 41 GHz. The single bias method exhibits a phase variation of  $570^\circ$ , but with high reflection loss (up to 24.7 dB) in regions where the phase changes rapidly. The smith chart is evident that in the proposed method, the reflection phase and magnitude exhibit a one-to-multiple correspondence with the LC permittivity. The reflection phase change remains similar to that of the single bias method, but independent control allows one phase to be mapped to multiple sets of  $(\epsilon_{r1}, \epsilon_{r2})$ . Consequently, the optimal reflection magnitude can be selected from these sets to achieve low reflection loss.

For demonstration, the optimum reflection magnitude across all phases at 41 GHz for both the single and dual bias voltage supply methods is depicted in Fig. 9(a). It can be observed that over the entire  $360^\circ$  phase change, the proposed dual bias method achieves a higher reflection magnitude compared to the single bias method, with a maximum improvement of 17 dB. Fig. 9(b) shows the calculated bistatic radar cross section (bRCS) for the two methods under  $0^\circ$  incidence. Up to a  $30^\circ$  beam steering angle, the proposed method exhibits a larger bRCS by up to 7.94 dB relative to the single bias method, thereby validating that the proposed approach reduces reflection loss and enables the LCIRS to reflect more energy toward the target direction.

### 4. Conclusion

In this paper, two element structures are proposed to reduce the reflection loss in LCIRS. The first approach introduces an air layer

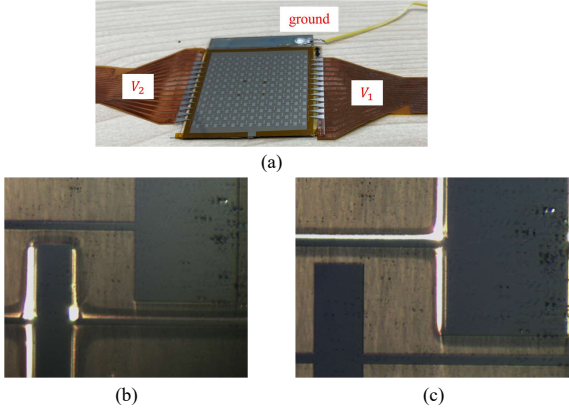


Fig. 7 (a) The prototype of the proposed LCIRS and the responses of LC under bias voltage (b) $V_1$  and (c)  $V_2$ .

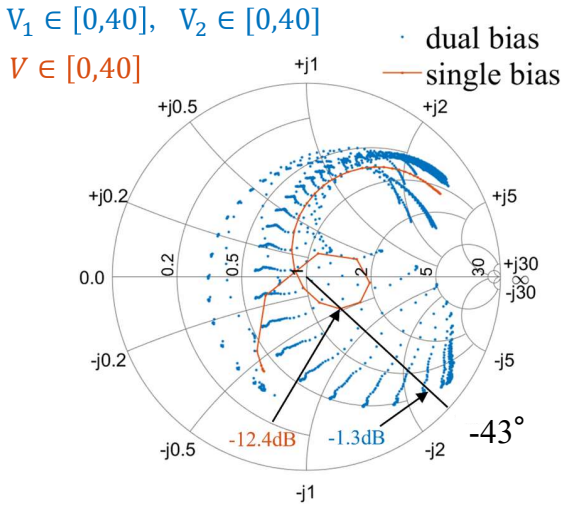
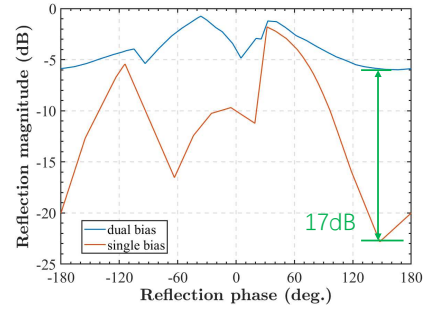


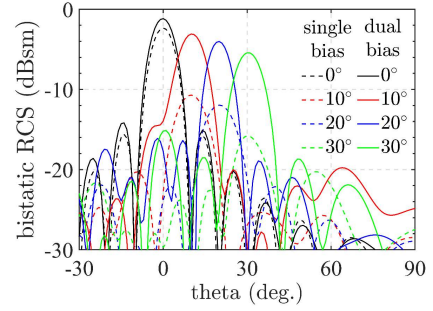
Fig. 8 (a) The reflection and (b) phase of the single bias voltage method. (c) The comparison of the two method in smith chart at 41 GHz.

beneath the LC layer. Theoretical analysis demonstrates a direct correlation between the effective permittivity of the air layer and the electric field within the LC layer, which in turn influences the reflection loss of the LCIRS. By modulating the thickness of the air layer, precise control over the effective permittivity is achieved, thereby reducing the reflection loss. A  $15 \times 15$  prototype array of the proposed LCIRS structure was fabricated, and experimental results indicated that the structure effectively reduces both the reflection loss and the variation in reflection magnitude, although the phase change decreases as the reflection loss is reduced.

To achieve independent control of the reflection magnitude and phase, a second element structure is proposed. In this design, the two resonant structures are connected to separate bias lines, realizing a dual-bias voltage supply. Consequently, the reflection magnitude and phase can be controlled independently. By selecting the optimum reflection magnitude for each phase, a significant reduction in reflection loss—up to 17 dB—is achieved without compromising the phase range. The proposed LCIRS structures offer advantages of low loss, wide phase change, cost-effectiveness, and ease of fabrication, making them promising candidates for practical applications.



(a)



(b)

Fig. 9 (a) The reflection and (b) phase of the single bias voltage method. (c) The comparison of the two method in smith chart at 41 GHz.

## 5. Acknowledgment

This work was supported by the Ministry of Internal Affairs and Communications in Japan (JPJ000254).

## References

- [1] W. Wu, K.-D. Xu, Q. Chen, T. Tanaka, M. Kozai, and H. Minami, "A wideband reflectarray based on single-layer magneto-electric dipole elements with 1-bit switching mode," *IEEE Trans. Antennas Propag.*, vol. 70, no. 12, pp. 12 346–12 351, 2022.
- [2] J. Han, L. Li, G. Liu, Z. Wu, and Y. Shi, "A wideband 1 bit  $12 \times 12$  reconfigurable beam-scanning reflectarray: Design, fabrication, and measurement," *IEEE Antennas Wireless Propag. Lett.*, vol. 18, no. 6, pp. 1268–1272, 2019.
- [3] W. Menzel, D. Pilz, and M. Al-Tikriti, "Millimeter-wave folded reflector antennas with high gain, low loss, and low profile," *IEEE Antennas Propag. Mag.*, vol. 44, no. 3, pp. 24–29, 2002.
- [4] S. Bildik, S. Dieter, C. Fritzsche, W. Menzel, and R. Jakoby, "Reconfigurable folded reflectarray antenna based upon liquid crystal technology," *IEEE Trans. Antennas Propag.*, vol. 63, no. 1, pp. 122–132, 2015.
- [5] P. Nayeri, F. Yang, and A. Z. Elsherbeni, *Reflectarray antennas: theory, designs, and applications*. John Wiley & Sons, 2018.
- [6] W. L. Stutzman and G. A. Thiele, *Antenna theory and design*. John Wiley & Sons, 2012.
- [7] C. A. Balanis, *Antenna theory: analysis and design*. John Wiley & Sons, 2016.
- [8] D. Pozar, *Microwave Engineering, 4th Edition*. Wiley, 2011.